The Astronomical Journal, 160:31 (15pp), 2020 July https://doi.org/10.3847/1538-3881/ab930b

A Search for Extra-tidal RR Lyrae in Globular Clusters NGC 5024 and NGC 5053

Chow-Choong Ngeow[1], Justin Belecki[2], Rick Burruss[2], Andrew J. Drake[3], Matthew J. Graham[3], David L. Kaplan[4], Thomas Kupfer[5], Ashish Mahabal[3,6], Frank J. Masci[7], Reed Riddle[2], Hector Rodriguez[2], and Ben Rusholme[7]
[1] Graduate Institute of Astronomy, National Central University, 300 Jhongda Road, 32001 Jhongli, Taiwan; cngeow@astro.ncu.edu.tw
[2] Caltech Optical Observatories, California Institute of Technology, Pasadena, CA 91125, USA
[3] Division of Physics, Mathematics, and Astronomy, California Institute of Technology, Pasadena, CA 91125, USA
[4] Center for Gravitation, Cosmology and Astrophysics, Department of Physics, University of Wisconsin–Milwaukee, Milwaukee, WI 53201, USA
[5] Kavli Institute for Theoretical Physics, University of California, Santa Barbara, CA 93106, USA
[6] Center for Data Driven Discovery, California Institute of Technology, Pasadena, CA 91125, USA
[7] IPAC, California Institute of Technology, 1200 E. California Boulevard, Pasadena, CA 91125, USA
Received 2020 April 9; revised 2020 May 8; accepted 2020 May 12; published 2020 June 18

Abstract

Recently, Kundu et al. reported that the globular cluster NGC 5024 (M53) possesses five extra-tidal RR Lyrae. In fact, four of them were instead known members of a nearby globular cluster NGC 5053. The status of the remaining extra-tidal RR Lyrae is controversial depending on the adopted tidal radius of NGC 5024. We have also searched for additional extra-tidal RR Lyrae within an area of $\sim$8 deg^2 covering both globular clusters. This includes other known RR Lyrae within the search area, as well as stars that fall within the expected range of magnitudes and colors for RR Lyrae (and yet outside the cutoff of two-thirds of the tidal radii of each globular cluster for something to be called extra-tidal) if they were extra-tidal RR Lyrae candidates for NGC 5024 or NGC 5053. Based on the the proper-motion information and their locations on the color–magnitude diagram, none of the known RR Lyrae belong to the extra-tidal RR Lyrae of either globular clusters. In the cases where the stars satisfied the magnitude and color ranges of RR Lyrae, analysis of time series data taken from the Zwicky Transient Facility do not reveal periodicities, suggesting that none of these stars are RR Lyrae. We conclude that there are no extra-tidal RR Lyrae associated with either NGC 5024 or NGC 5053 located within our search area.

Unified Astronomy Thesaurus concepts: Globular star clusters (656); RR Lyrae variable stars (1410); Tidal tails (1701); Sky surveys (1464)

1. Introduction

As an ancient population that is orbiting around our Galaxy in its halo, globular clusters could leave tidal tails along their orbits. Indeed, tidal tails have already been detected in some globular clusters such as Palomar 5 (Odenkirchen et al. 2001; Rockosi et al. 2002), NGC 5466 (Belokurov et al. 2006), Palomar 1 (Niederste-Ostholt et al. 2010), Palomar 14 (Sollima et al. 2011), Palomar 15 (Myeong et al. 2017), Eridanus (Myeong et al. 2017), NGC 7492 (Navarrete et al. 2017), and M5 (Grillmair 2019). The existence of tidal tails from globular clusters were also supported from theoretical modeling and simulations (for examples, see Combes et al. 1999; Yim & Lee 2002; Dehnen et al. 2004; Capuzzo Dolcetta et al. 2005; Lee et al. 2006; Fellhauer et al. 2007; Montuori et al. 2007; Hozumi & Burkert 2015). The tidally stripped stars in the tails are preferentially low-mass stars (Combes et al. 1999; Baumgardt & Makino 2003), which could include RR Lyrae (Jordi & Grebel 2010). As low-mass high-amplitude pulsating stars, RR Lyrae can be easily identified from time domain surveys based on their characteristic light-curve shapes. RR Lyrae are precise distance indicators hence distances to the tidal tails can be constrained if the extra-tidal RR Lyrae can be found in the associated tidal tails. Furthermore, RR Lyrae are more luminous than the main-sequence stars at similar mass, hence they can be used to reveal the presence of tidal tails around distant globular clusters. In this regard, it is important and interesting to search for extra-tidal RR Lyrae associated with globular clusters. As demonstrated in Kunder et al. (2018) and Minniti et al. (2018), findings of extra-tidal RR Lyrae could be used to constrain the history of orbital motion and the dynamic processes of the parent globular clusters.

Extra-tidal RR Lyrae stars have been found around several globular clusters. Based on wide-field imaging, Fernández-Trincado et al. (2015) reported about a dozen RR Lyrae located at a distance similar to ω Centauri (NGC 5139), which are also located outside the tidal radius (r_t) of this cluster. However the authors suggested that they are unlikely to be associated with the tidal debris of ω Centauri. In contrast, eight extra-tidal RR Lyrae candidates were found for NGC 6441, as their radial velocities are consistent with the cluster and they are located between 1 and 3 tidal radii from the cluster (Kunder et al. 2018). Using Gaia Data Release 2 (DR2; Gaia Collaboration et al. 2016, 2018a) data, Minniti et al. (2018) discovered that there is an excess of RR Lyrae outside the tidal radius of M62 (NGC 6266), which the authors interpreted as tidally stripped RR Lyrae while the cluster is crossing the Galactic bulge. Recently, Price-Whelan et al. (2019) found 17 RR Lyrae that most likely belong to the stellar stream of Palomar 5, with a few of them previously identified as potential members (Vivas et al. 2001; Wu et al. 2005; Vivas & Zinn 2006). An independent search of RR Lyrae in the stellar stream of Palomar 5 was also performed in Ibata et al. (2017).

In addition to the individual globular clusters, Kundu et al. (2019) performed a systematic search for extra-tidal RR Lyrae around globular clusters with Gaia DR2 data and the Gaia DR2 RR Lyrae Catalog (Clementini et al. 2019). Out of the 56 globular clusters, the authors identify 11 globular clusters possessing extra-tidal RR Lyrae based on their positions (out to three times the tidal radius of each cluster), proper motions, and

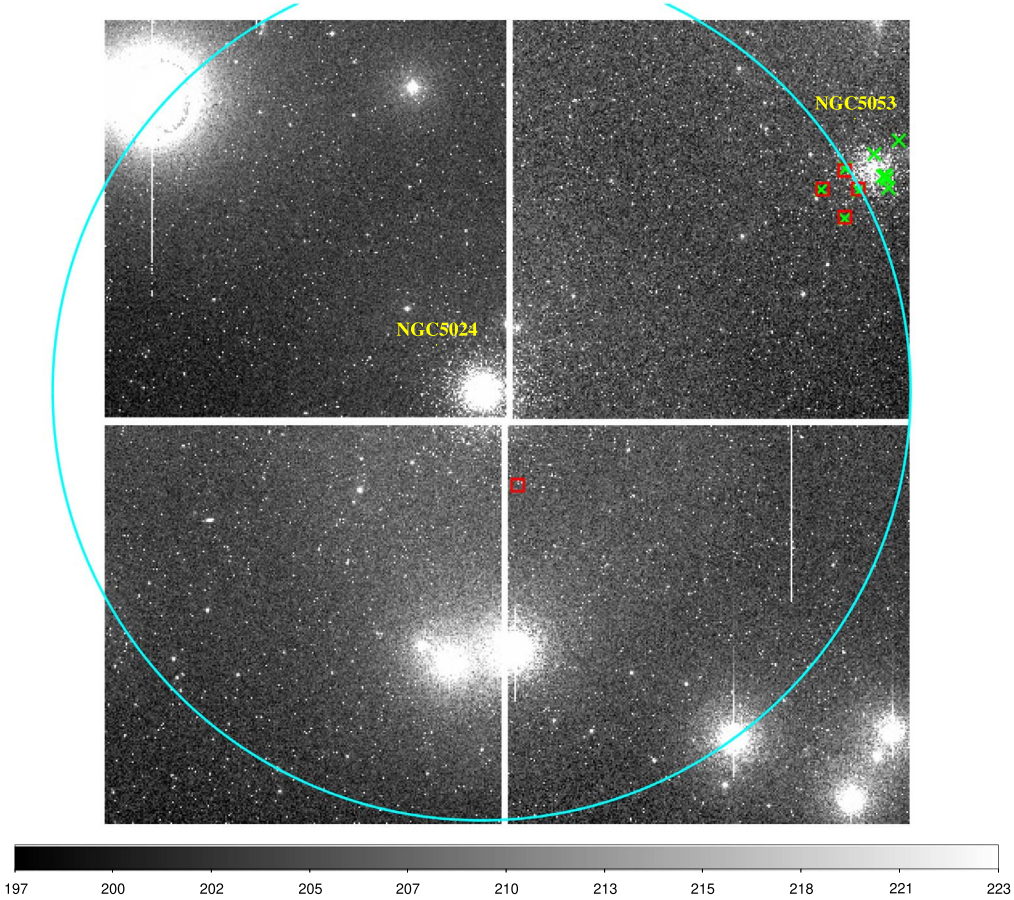

Figure 1. ZTF mosaic (see Section 3 for more details on ZTF) *r*-band reference images, with ZTFID of 1573 and CCD 15, that display the positions of NGC 5024 and NGC 5053. The cyan circle indicates the radius of $3 \times r_t$ of NGC 5024 as adopted in Kundu et al. (2019). The red squares represent the extra-tidal RR Lyrae identified in Kundu et al. (2019), while the green crosses are known RR Lyrae of NGC 5053 taken from Clement's Catalog (Clement et al. 2001; Clement 2017).

locations in the color–magnitude diagrams (CMDs). Among these 11 globular clusters, six globular clusters have one extra-tidal RR Lyrae while another three clusters have two (including Palomar 5). The remaining two globular clusters, NGC 5024 and NGC 3201, were found to have 5 and 13 extra-tidal RR Lyrae, respectively. The extra-tidal RR Lyrae in NGC 5024 merit further discussion, as four of them are located on one side of the cluster at a (projected) distance near three times the tidal radius (that is, 55′.1). This is close to a nearby globular cluster: NGC 5053 located at a projected distance of ∼57′.7 away from NGC 5024. In fact, these four extra-tidal RR Lyrae of NGC 5024 are instead known RR Lyrae from NGC 5053 as listed in the Updated Catalog of Variable Stars in Globular Clusters (Clement et al. 2001; Clement 2017, hereafter Clement's Catalog), as illustrated in Figure 1. Hence the number of extra-tidal RR Lyrae in NGC 5024 should be reduced to one.

Since NGC 5053 is not included in the list of 56 globular clusters given in Kundu et al. (2019), it may contain additional (uncatalogued) extra-tidal RR Lyrae. Separately, we wish to ascertain whether there could be more extra-tidal RR Lyrae from NGC 5024, in addition to the one that was identified and discussed above. The goal of this work is to search for (additional) extra-tidal RR Lyrae in NGC 5024 and NGC 5053, given the close proximity of these two globular clusters in the sky. Note that based on imaging observations using the Canada–Hawaii–France Telescope, Chun et al. (2010) reported there was a tidal bridge feature between NGC 5024 and NGC 5053. However, such a tidal bridge feature was not confirmed in Jordi & Grebel (2010). Nevertheless, Jordi & Grebel (2010) found extra-tidal halos in both globular clusters, and confirmed the detection of a tidal tail for NGC 5053 reported in Lauchner et al. (2006). On the other hand, a possible tidal tail could be present for NGC 5024 (Beccari et al. 2008) but no conclusive result can be determined.

In Section 2, we compile a list of known and candidate RR Lyrae collected from the literature, and determine if any of them are extra-tidal RR Lyrae. In Section 3, we search for potential new extra-tidal RR Lyrae using Gaia DR2 data and time series data taken from the Zwicky Transient Facility (ZTF). The conclusion of this work is presented in Section 4.

2. Known and Candidate RR Lyrae in the Vicinity of the Clusters

The tidal radii r_t of NGC 5024 and NGC 5053 were adopted from de Boer et al. (2019) as $22'.8 \pm 1'.4$ and $15'.2 \pm 3'.3$, respectively. For consistency, these tidal radii were based on the fitted spherical potential escapers stitched (SPES) model[8] to the number density profile constructed from Gaia DR2 and literature data, converted from parsec to arcminute using the

[8] In the case of NGC 5053, even though the Wilson model is a better fit to its number density (de Boer et al. 2019), the derived tidal radius from the Wilson model, $18'.1 \pm 1'.5$, is in good agreement with the value based on the SPES model.

Table 1
Known RR Lyrae in NGC 5024 and NGC 5053 (Group A)

Name[a]	α_{J2000}	δ_{J2000}	Δ_{5024}[b]	Δ_{5053}[b]	Gaia DR2 ID	G[c]	$B_p - R_p$[c]	pmRA[d]	pmDE[d]
NGC 5024 V61	198.22967	18.17014	0.12	57.76	3938022017256098432	−99.99	−99.99	0.224 ± 0.652	0.351 ± 0.449
NGC 5024 V57	198.23150	18.16617	0.14	57.56	3938022017253298816	16.620	−99.99	0.820 ± 0.549	−3.508 ± 0.425
NGC 5024 V63	198.23454	18.16686	0.26	57.43	3937271394410272128	−99.99	−99.99	0.596 ± 0.657	0.233 ± 0.479
NGC 5024 V72	198.23308	18.16453	0.27	57.43	3937271394411045760	−99.99	−99.99	2.074 ± 0.339	0.021 ± 0.231
NGC 5024 V71	198.22658	18.16500	0.28	57.77	3938022017255714688	−99.99	−99.99	−2.708 ± 0.789	−1.737 ± 0.813
NGC 5024 V91	198.22342	18.17044	0.41	58.08	3938022017256046592	−99.99	−99.99	2.884 ± 0.445	1.536 ± 0.333
NGC 5024 V53	198.23263	18.17544	0.46	57.77	3938022395210336128	−99.99	−99.99	−99.99	−99.99
NGC 5024 V54	198.22629	18.17542	0.49	58.09	3938022017256105344	16.633	−99.99	−3.039 ± 0.587	5.163 ± 0.476
NGC 5024 V62	198.22500	18.17494	0.50	58.14	3938022017255910528	−99.99	−99.99	0.153 ± 0.687	−0.421 ± 0.481
NGC 5024 V46	198.22721	18.17694	0.55	58.09	3938022017255848704	16.622	0.544	−0.734 ± 0.288	−1.025 ± 0.166
NGC 5024 V52	198.23300	18.17697	0.55	57.80	3938022395212860928	16.782	−99.99	0.783 ± 0.392	−1.968 ± 0.438
NGC 5024 V58	198.23167	18.15861	0.58	57.33	3937271394411059072	16.665	0.564	0.910 ± 0.345	−0.307 ± 0.238
NGC 5024 V45	198.22983	18.15761	0.63	57.39	3937271394410013312	16.640	0.560	−0.027 ± 0.259	−0.525 ± 0.184
NGC 5024 V60	198.23742	18.16014	0.63	57.09	3937271394411025920	16.385	−99.99	−99.99	−99.99
NGC 5024 V64	198.21883	18.17014	0.66	58.31	3938022017255783424	−99.99	−99.99	−2.644 ± 1.265	1.637 ± 0.863
NGC 5024 V55	198.22275	18.17683	0.67	58.30	3938022085972624768	16.484	−99.99	0.001 ± 0.253	−0.828 ± 0.144
NGC 5024 V56	198.22371	18.15722	0.75	57.69	3937271360050576512	16.778	−99.99	−2.101 ± 0.442	−3.017 ± 0.257
NGC 5024 V92	198.22879	18.18064	0.75	58.12	3938022395213189248	−99.99	−99.99	−1.276 ± 0.402	−1.295 ± 0.238
NGC 5024 V59	198.23608	18.15578	0.82	57.03	3937271394411208192	−99.99	−99.99	0.108 ± 0.638	−2.325 ± 0.489
NGC 5024 V44	198.21525	18.16683	0.86	58.39	3938021982896346240	16.718	0.470	−0.399 ± 0.235	−2.076 ± 0.129
NGC 5024 V51	198.23996	18.18047	0.92	57.56	3938022395210481408	−99.99	−99.99	1.433 ± 0.235	−0.515 ± 0.135
NGC 5024 V43	198.22117	18.18208	0.98	58.54	3938022085975189504	16.664	0.580	0.285 ± 0.225	−0.592 ± 0.164
NGC 5024 V31	198.24821	18.16803	1.03	56.78	3937271772365640960	16.608	0.605	−0.807 ± 0.186	−1.311 ± 0.128
NGC 5024 V41	198.23646	18.18569	1.11	57.89	3938022395210877312	16.760	0.378	0.203 ± 0.180	−1.318 ± 0.119
NGC 5024 V42	198.21058	18.17225	1.15	58.78	3938022051615475712	16.640	0.621	−2.918 ± 0.340	−1.781 ± 0.190
NGC 5024 V37	198.21783	18.18483	1.22	58.78	3938022085972862848	16.693	0.622	−0.247 ± 0.168	−1.229 ± 0.115
NGC 5024 V09	198.25029	18.15697	1.33	56.35	3937271321396679936	16.777	0.632	−0.447 ± 0.193	−1.355 ± 0.144
NGC 5024 V18	198.20250	18.17033	1.58	59.13	3938022047320224768	16.822	0.406	−0.580 ± 0.312	−1.941 ± 0.217
NGC 5024 V08	198.25171	18.18475	1.58	57.11	3938022429571836288	16.772	0.534	0.858 ± 0.320	−1.812 ± 0.191
NGC 5024 V40	198.23276	18.19852	1.83	58.46	3938022498291497088	16.843	0.354	−0.051 ± 0.166	−1.600 ± 0.113
NGC 5024 V07	198.25363	18.19165	1.94	57.23	3938022429572023424	16.844	0.562	0.440 ± 0.221	−1.190 ± 0.166
NGC 5024 V24	198.19700	18.15900	1.97	59.09	3938021948535632768	−99.99	−99.99	−0.077 ± 0.168	−1.389 ± 0.110
NGC 5024 V06	198.26630	18.17220	2.07	56.01	3937271733713546624	16.706	0.614	0.027 ± 0.229	−1.650 ± 0.160
NGC 5024 V25	198.26841	18.17703	2.24	56.05	3937271733710749056	16.720	0.544	−0.176 ± 0.192	−1.622 ± 0.147
NGC 5024 V23	198.25978	18.14332	2.25	55.49	3937271119532519808	16.772	0.430	−0.397 ± 0.242	−2.690 ± 0.180
NGC 5024 V32	198.19893	18.14327	2.33	58.56	3938021841161792640	16.758	0.451	−0.008 ± 0.159	−1.517 ± 0.121
NGC 5024 V10	198.19053	18.18207	2.41	60.06	3938022253478651392	16.722	0.478	−0.327 ± 0.175	−1.294 ± 0.115
NGC 5024 V38	198.23812	18.12791	2.46	56.15	3937270977799285376	16.714	0.597	−0.646 ± 0.159	−1.428 ± 0.104
NGC 5024 V03	198.21410	18.12926	2.51	57.41	3937271149597965312	16.818	0.493	−0.341 ± 0.153	−1.174 ± 0.107
NGC 5024 V29	198.26779	18.14637	2.51	55.17	3937271497489647616	−99.99	−99.99	−0.482 ± 0.177	−1.250 ± 0.128
NGC 5024 V11	198.18912	18.15054	2.57	59.25	3938021909878970752	16.765	0.533	−0.151 ± 0.173	−1.178 ± 0.118
NGC 5024 V47	198.21008	18.20686	2.59	59.83	3938022738809664000	16.742	0.372	−0.245 ± 0.174	−1.042 ± 0.130
NGC 5024 V33	198.18278	18.17024	2.71	60.12	3938022154692482944	16.729	0.673	0.086 ± 0.179	−1.397 ± 0.126
NGC 5024 V01	198.23478	18.12049	2.87	56.12	3937270982093531648	16.770	0.518	0.249 ± 0.169	−1.560 ± 0.114
NGC 5024 V19	198.27926	18.15730	2.87	54.92	3937271531849398400	16.802	0.434	−0.111 ± 0.187	−1.393 ± 0.143
NGC 5024 V35	198.26011	18.21047	3.06	57.50	3938022567010985984	16.824	0.446	−0.374 ± 0.182	−1.167 ± 0.139
NGC 5024 V02	198.20952	18.11687	3.30	57.31	3937269676423468672	16.788	0.372	−0.609 ± 0.194	−1.337 ± 0.116
NGC 5024 V04	198.18288	18.12395	3.78	58.87	3938020367987656320	16.800	0.432	0.191 ± 0.163	−1.351 ± 0.106
NGC 5024 V17	198.16807	18.19833	3.98	61.66	3938023082407017088	16.806	0.465	0.244 ± 0.170	−1.226 ± 0.113
NGC 5024 V16	198.19250	18.11085	4.06	58.04	3937269642063727360	16.871	0.345	−0.195 ± 0.170	−1.423 ± 0.122
NGC 5024 V27	198.17261	18.12322	4.25	59.38	3938020333627916928	16.723	0.593	−0.515 ± 0.154	−1.178 ± 0.109
NGC 5024 V34	198.19045	18.10722	4.30	58.05	3937269642063726080	−99.99	−99.99	−0.123 ± 0.174	−1.372 ± 0.125
NGC 5024 V36	198.26373	18.25287	5.43	58.72	3939524087576094848	16.825	0.413	−0.065 ± 0.186	−1.354 ± 0.144
NGC 5024 V15	198.30162	18.23205	5.59	56.23	3939523915777402368	16.847	0.364	−0.511 ± 0.197	−1.091 ± 0.164
NGC 5024 V05	198.16285	18.09508	5.83	59.19	3937269573344246528	16.725	0.577	−0.158 ± 0.162	−1.170 ± 0.103
NGC 5024 V26	198.14894	18.08894	6.64	59.78	3937269191089937536	16.753	0.448	−0.278 ± 0.173	−1.519 ± 0.113
NGC 5024 V20	198.28781	18.07121	6.68	52.10	3937269809565198720	16.801	0.449	−0.107 ± 0.169	−1.505 ± 0.130
NGC 5024 V14	198.33562	18.11195	6.89	50.79	3937270359321073792	16.784	0.488	−0.016 ± 0.180	−1.541 ± 0.154
NGC 5024 V28	198.17547	18.27716	7.25	63.72	3938026930697675648	16.715	0.506	−0.210 ± 0.158	−1.241 ± 0.110
NGC 5024 V21	198.35868	18.16208	7.33	51.20	3938772017327358336	16.818	0.418	−0.586 ± 0.198	−1.318 ± 0.150
NGC 5024 V12	198.34930	18.22126	7.50	53.63	3938773048119562496	16.742	0.511	−0.258 ± 0.171	−1.355 ± 0.131
NGC 5024 V30	198.25068	18.03440	8.11	53.16	3937268160297720576	16.824	0.479	−0.182 ± 0.147	−1.464 ± 0.116
NGC 5024 V13	198.36767	18.08693	9.23	48.46	3937267133802945024	16.718	0.497	0.116 ± 0.209	−1.422 ± 0.168
NGC 5024 V48	198.30983	18.36777	12.81	60.85	3939527386110983424[e]	16.800	0.392	−0.085 ± 0.166	−1.636 ± 0.117

Table 1
(Continued)

Name[a]	α_{J2000}	δ_{J2000}	Δ_{5024}[b]	Δ_{5053}[b]	Gaia DR2 ID	G[c]	$B_p - R_p$[c]	pmRA[d]	pmDE[d]
NGC 5053 V10	199.13554	17.71290	58.45	1.50	3938494459361028992	−99.99	−99.99	−0.278 ± 0.213	−0.727 ± 0.146
NGC 5053 V08	199.14179	17.71116	58.82	1.78	3938494463656186880	16.620	0.435	−0.367 ± 0.156	−1.166 ± 0.105
NGC 5053 V04	199.11674	17.66565	58.91	2.09	3938493948260097024	16.501	−99.99	−0.495 ± 0.140	−1.370 ± 0.128
NGC 5053 V06	199.14425	17.71869	58.73	2.11	3938494566735402880	16.695	0.333	−0.192 ± 0.150	−1.504 ± 0.108
NGC 5053 V03	199.14842	17.73773	58.43	3.03	3938682273986049792	16.575	0.537	−0.378 ± 0.135	−1.252 ± 0.101
NGC 5053 V07	199.08220	17.74399	54.89	3.16	3938682445784738688[e]	16.549	0.371	−0.318 ± 0.158	−1.390 ± 0.106
NGC 5053 V02	199.05154	17.69631	54.77	3.51	3938681827309432448[e]	16.609	0.460	−0.145 ± 0.147	−1.286 ± 0.107
NGC 5053 V05	199.17174	17.63628	62.52	5.10	3938492883108232960	16.513	0.617	−0.330 ± 0.132	−1.341 ± 0.101
NGC 5053 V01	198.99724	17.74100	50.73	7.05	3938682995540541440[e]	16.526	0.545	−0.355 ± 0.151	−1.350 ± 0.095
NGC 5053 V09	199.04957	17.80299	51.64	7.15	3938686637672823424[e]	16.523	0.618	−0.377 ± 0.139	−1.149 ± 0.092

Notes.
[a] Known RR Lyrae adopted from Clement's Catalog. The number −99.99 means no data.
[b] Δ represents the angular distance, in arcminutes, for a given RR Lyrae to the center of the cluster.
[c] Intensity mean magnitudes and colors taken from the Gaia DR2 RR Lyrae Catalog (i.e., the `gaiadr2.vary_rrlyrae` Table).
[d] Proper motions in mas yr^{-1} taken from Gaia DR2 main catalog.
[e] Extra-tidal RR Lyrae for NGC 5024 identified in Kundu et al. (2019).

distances provided in Harris et al. (1996, 2010; the 2010 edition, hereafter Harris Catalog),[9] where the distances to NGC 5024 and NGC 5053 are 17.9 kpc and 17.4 kpc, respectively. Because the areas enclosed by the $3r_t$ regions for these two clusters overlapped, we defined a circle with a radius of 1.°6, centered at $(\alpha, \delta)_{J2000} = (198.48568, +17.90798)°$ (see Figure 4), to search and identify RR Lyrae from the literature within this ∼8 deg^2 area.

We collected known and candidate RR Lyrae located within this circle from various catalogs. These catalogs include Clement's Catalog (NGC 5024: 64 stars; NGC 5053: 10 stars), the catalog from the American Association of Variable Star Observers (AAVSO) International Variable Star Index (VSX; Watson et al. 2006, 55 stars), and those from Sesar et al. (2017, 91 stars). The primary recent sources for RR Lyrae compiled in Clement's Catalogs are Arellano Ferro et al. (2011) for NGC 5024 and Nemec (2004) for NGC 5053, respectively. We selected all entries in Sesar et al. (2017) within the predefined circle regardless of the final classification scores `S3ab` and `S3c`, hence some of them with low scores were considered RR Lyrae candidates.[10] All of the above were queried via the `SIMBAD`'s `VizieR` service. We have also searched the Gaia DR2 RR Lyrae Catalog (Clementini et al. 2019, the `gaiadr2.vary_rrlyrae` Table; 79 stars) and RR Lyrae in the Gaia DR2 high-amplitude pulsating stars Catalog (Rimoldini et al. 2019, the `gaiadr2.vari_classifier_result` Table; 70 stars) via the astronomical data query language (ADQL) interface from the Gaia archive.[11] We combined the query results from these two tables, using the `source_id`, for a total of 80 RR Lyrae from Gaia DR2 (hereafter GaiaDR2RRL catalog). Finally, we merged all of the above catalogs, using positional matching, to create a master catalog that contains 125 RR Lyrae and candidates within the circle mentioned earlier.

A further examination of these 125 RR Lyrae revealed that 29 RR Lyrae candidates do not have any counterparts in either Clement's Catalog, the VSX catalog, or the GaiaDR2RRL catalog. All of them have classification scores `S3ab` and `S3c` smaller than 0.52 in the Sesar et al. (2017) catalog, with brightness fainter than ∼18.5 mag in the r band or Gaia's G band. We believe they are either misclassified or background RR Lyrae that are unrelated to NGC 5024 and NGC 5053 (the RR Lyrae in these two globular clusters should be brighter than ∼17.5 mag in the r or G band), hence we removed them from our master catalog (a detailed investigation of them is beyond the scope of this work). The remainder of the 96 RR Lyrae in our master catalog will be divided into two groups, and analyzed with criteria similar to those outlined in Kundu et al. (2019), as presented in the following subsections.

2.1. Group A: Known Members in NGC 5024 and NGC 5053

In Table 1 we summarize the basic information for the 74 known RR Lyrae located in NGC 5024 and NGC 5053. Positions of these RR Lyrae in the CMDs are presented in Figure 2. The stars, including the extra-tidal RR Lyrae identified in Kundu et al. (2019), are undoubtedly RR Lyrae stars as they are located as expected on the horizontal branch on the CMDs of these two globular clusters. The four extra-tidal RR Lyrae that belong to NGC 5053 (green points in Figure 2), but were misidentified as members of NGC 5024, are well positioned on the horizontal branch for the NGC 5053's CMD, but shifted upward in the case of NGC 5024's CMD (due to difference in the distance of these two globular clusters). In contrast, the one remaining extra-tidal RR Lyrae of NGC 5024 fits well to the horizontal branch of NGC 5024 (cyan point in Figure 2).

To further evaluate the associations of these known RR Lyrae to the two globular clusters, we compared their proper motions with the measured proper motions of NGC 5024 and NGC 5053 in Figure 3. The circles in this figure denote the boundaries of the proper motions such that RR Lyrae located within the circles are considered to have proper motions consistent with the globular clusters. It is worth pointing out that the proper motions of the two globular clusters, as measured in Gaia Collaboration et al. (2018b), are close to each other: the proper motions in

[9] We thank T. de Boer for verifying this.
[10] The scores have a value between 0 and 1, where 1 represents the star having a very high probability of being an RR Lyrae, and 0 if the star is not classified as an RR Lyrae. These scores have an associated level of purity and completeness as described in Sesar et al. (2017). For example, `S3ab > 0.8` implies the underlying star is an ab-type RR Lyrae with purity of 91% and completeness of 77% at ∼80 kpc.
[11] http://gea.esac.esa.int/archive/

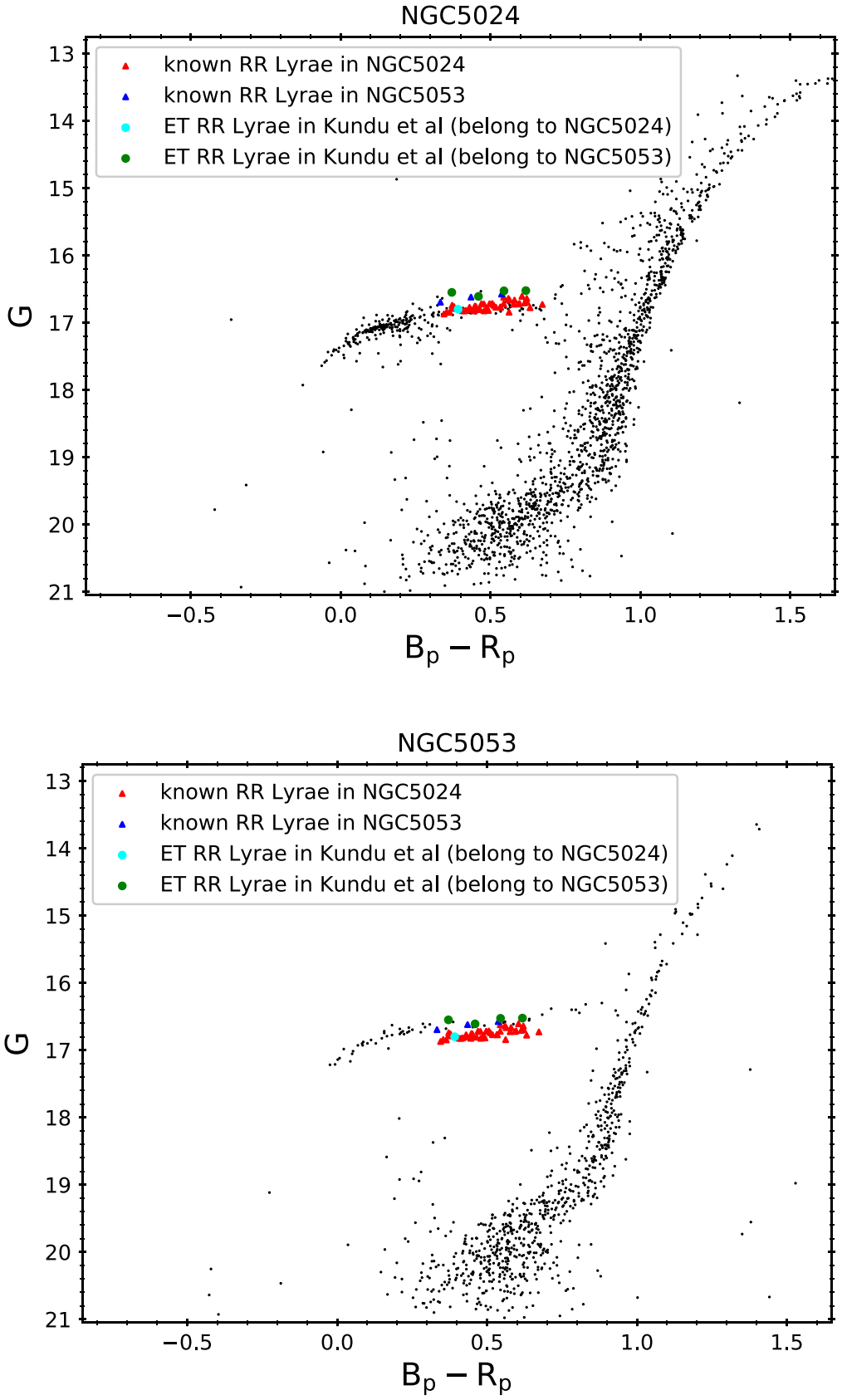

Figure 2. The clean color–magnitude diagram (CMD) for NGC 5024 (left panel) and NGC 5053 (right panel) based on Gaia photometry. The color coded symbols represent the known RR Lyrae, based on Clement's Catalog, in these two globular clusters. Extra-tidal RR Lyrae identified in Kundu et al. (2019) are abbreviated as ET RR Lyrae (four of them belong to NGC 5053 and are shown as large green points). Procedures for obtaining the clean CMD are explained in Appendix A. The CMD for NGC 5053 is similar to those presented in Sarajedini & Milone (1995).

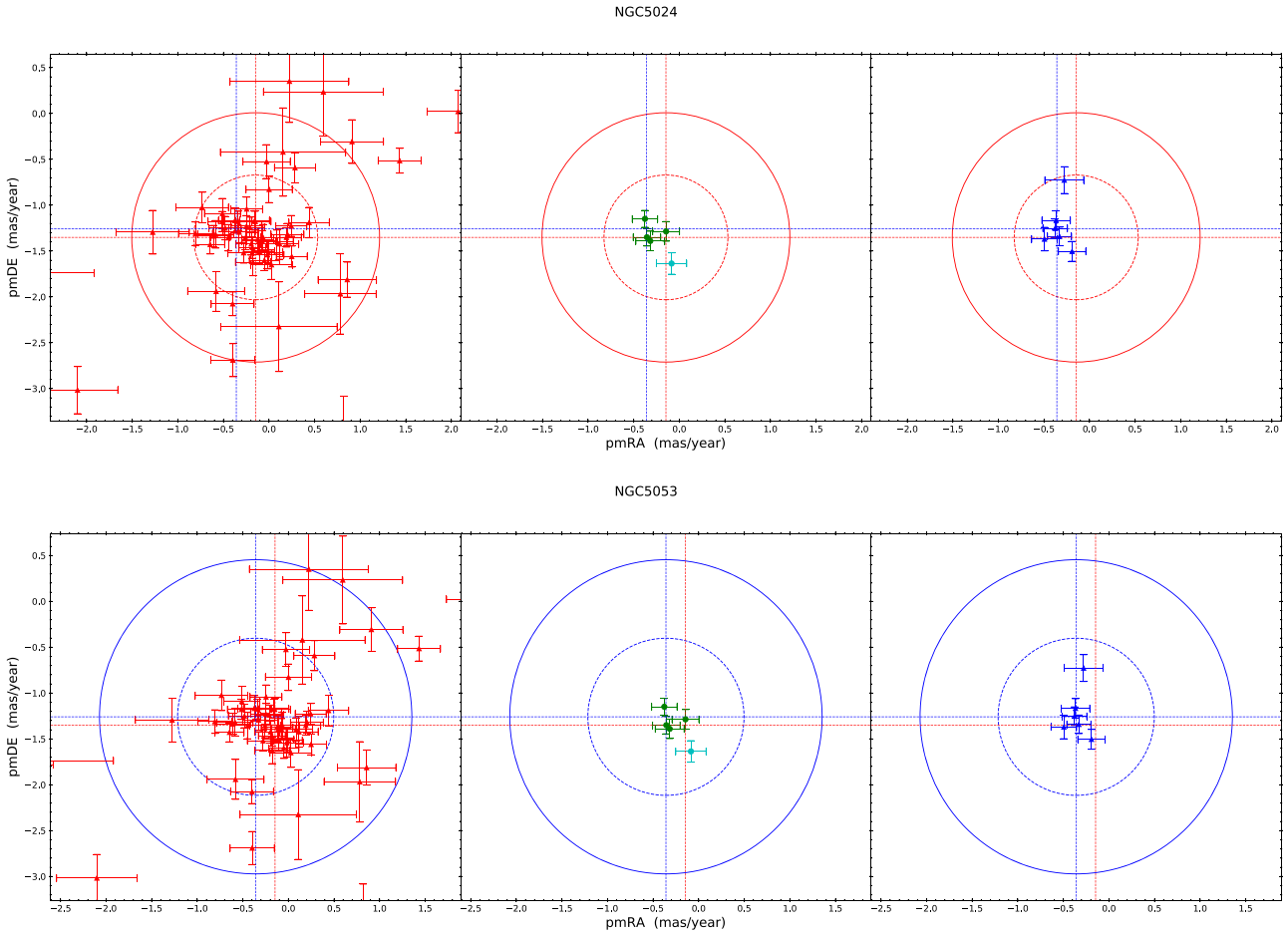

Figure 3. Comparisons of the proper motions of the known RR Lyrae in NGC 5024 and NGC 5053 to the values of the two globular clusters themselves. The red and blue dashed lines in each panel represent the measured proper motions of NGC 5024 and NGC 5053, respectively, adopted from Gaia Collaboration et al. (2018b). The dashed and solid circles represent the selection criteria of $\Delta_{\rm PM} = {\rm pmT}/2$ and $\Delta_{\rm PM} = {\rm pmT}$, respectively; see Appendix A for the definitions of $\Delta_{\rm PM}$ and pmT. The colored symbols are same as in Figure 2. For better visualization, we divided the known RR Lyrae to those belonging to NGC 5024 (left panels; red points), NGC 5053 (right panels; blue points), and the extra-tidal RR Lyrae (middle panels; green and cyan points).

R.A. are $\mathrm{pmRA}_c^{5024} = -0.1466 \pm 0.0045$ (mas yr^{-1}) and $\mathrm{pmRA}_c^{5053} = -0.3591 \pm 0.0071$ (mas yr^{-1}), while in the decl. they are $\mathrm{pmDE}_c^{5024} = -1.3514 \pm 0.0032$ (mas yr^{-1}) and $\mathrm{pmDE}_c^{5053} = -1.2586 \pm 0.0048$ (mas yr^{-1}). Therefore, it is difficult to associate these RR Lyrae with either of the globular clusters based on proper motions alone. Figure 3 reveals that this is indeed the case: proper motions of the known RR Lyrae in NGC 5024 are consistent with the proper motions of both globular clusters (left panels of Figure 3),[12] and a similar situation holds for the RR Lyrae in NGC 5053 (right panels of Figure 3). For the five extra-tidal RR Lyrae identified in Kundu et al. (2019), their proper motions are fully consistent with either NGC 5024 or NGC 5053 (middle panels of Figure 3). This explains why Kundu et al. (2019) would include the four RR Lyrae from NGC 5053 as the extra-tidal RR Lyrae for NGC 5024 based on the proper-motion analysis.

Finally, we comment on the only extra-tidal RR Lyrae of NGC 5024, V48, which is located 12.′81 away from NGC 5024. In Kundu et al. (2019), the adopted tidal radius of NGC 5024 is 18.′37, hence two-thirds of it is 12.′25 which puts V48 at a borderline to be considered an extra-tidal RR Lyrae. In contrast, two-thirds of the tidal radius adopted in this work is 15.′20, then V48 will no longer be an extra-tidal RR Lyrae of NGC 5024. The cutoff of two-thirds of the tidal radius was based on the criterion defined in Kundu et al. (2019), at which the authors did not elaborate the reason for adopting such cutoff radius (also, see the discussion in Section 4). Other tidal radii, in arcminutes, of NGC 5024 that can be found in the literature range from 14.79 ± 7.19 (Jordi & Grebel 2010), 16.25 (McLaughlin & van der Marel 2005), 16.91 (Kharchenko et al. 2013), 21.85 (Peterson & King 1975), 21.87 ± 0.53 (Lehmann & Scholz 1997), and 22.48 (Trager et al. 1995).[13] Therefore, depending on the adopted tidal radius, V48 could be either an extra-tidal RR Lyrae or not.

2.2. Group B: Other Known RR Lyrae in the Vicinity

For the remaining 22 RR Lyrae, 17 and 5 of them are known RR Lyrae from the VSX and GaiaDR2RRL catalogs, respectively. Among the five RR Lyrae from the GaiaDR2RRL

[12] There are few NGC 5024 RR Lyrae located outside the circles in left panels of Figure 3, indicating a possibility that they may not belong to NGC 5024. However they are all located within ∼2.′3 from the center of NGC 5024. The investigation of their memberships with NGC 5024 is not main scope of this paper, hence we will not study them in detail further.

[13] Values taken from Table 4 of Lehmann & Scholz (1997).

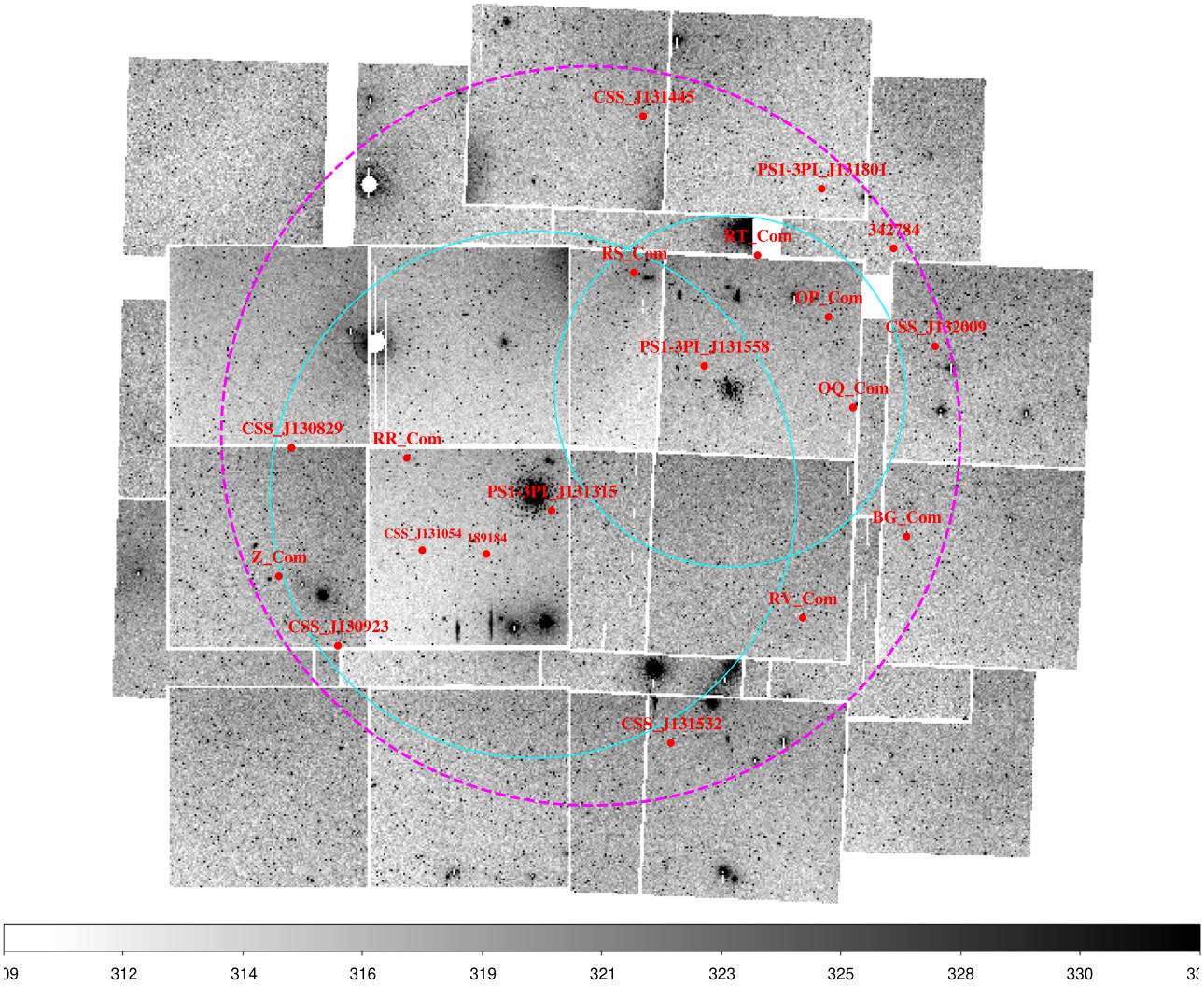

Figure 4. Locations of the 17 known RR Lyrae in Group B on the (inverted) ZTF mosaic *r*-band reference images. Two cyan circles indicate the $3r_t$ radii for both globular clusters, while the dashed magenta circle represents the adopted search radius of 1.°6. For clarity, names for some of the RR Lyrae were shortened (see Table 2) and for the two RR Lyrae listed in the GaiaDR2RRL catalog only the last six digits were shown.

catalog, three of them are located within 2′of the center of NGC 5024.[14] Two of them have $G > 19.7$ mag hence they could be the background stars, and the RR Lyrae with the Gaia DR2 ID of 3938022017256004352 has a *G*-band magnitude of 16.538 ± 0.001 mag. This RR Lyrae could be a new member of NGC 5024, but no proper-motion information available in the Gaia DR2 main catalog. Nevertheless, we excluded these three RR Lyrae in this work. The locations of other 19 RR Lyrae with respect to NGC 5024 and NGC 5053 are shown in Figure 4. These RR Lyrae were further grouped into four subgroups based on their locations relative to the two globular clusters, as summarized in Table 2. The comparisons of their proper motions to those of NGC 5024 and NGC 5053, as well as their positions on the CMD, are displayed in Figure 5. Two RR Lyrae, PS1-3PI J131315.63 + 181410.1 (or PS1-3PI J131315 in Table 2) and Gaia DR2 ID 3938041533584189184, were found to be misidentified RR Lyrae (see Appendix B for more details).

Seven RR Lyrae appeared to have proper motions consistent with either of the globular clusters as shown in the left panels of Figure 5, and they also satisfied the proper-motion criterion given in Kundu et al. (2019). However, these seven RR Lyrae are all fainter than $G \sim 18$ mag in the CMD,[15] as presented in right panel of Figure 5, hence they most likely belong to the background population of RR Lyrae in the Galactic halo. In contrast, three RR Lyrae are located in the magnitude range of $16.0 < G < 17.5$, enclosing the expected magnitudes of the horizontal branch stars in NGC 5024 and NGC 5053. CSS J130923.9 + 185016 is located right on top of the horizontal branch of NGC 5053 but it is closer to NGC 5024 on the sky. Similarly, OP Com seems to match with the horizontal branch of NGC 5024 but it is located near NGC 5053. Proper motions of these two RR Lyrae exhibit a large deviation relative to either of the globular clusters and hence they do not appear to be members or extra-tidal RR Lyrae of these two clusters. The

[14] The Gaia DR2 ID for these three RR Lyrae are: 3938022017256004352, 3938022085975309952, and 3938022463930328960.

[15] In the case of PS1-3PI J131315.63 + 181410.1, there is no *G*-band intensity mean magnitude given in the `gaiadr2.vary_rrlyrae` table. Nevertheless the Gaia DR2 main catalog listed a value of $G = 20.222 \pm 0.007$ mag for this RR Lyrae.

Table 2
Known RR Lyrae in the Vicinity of NGC 5024 and NGC 5053 (Group B)

VSX Name	α_{J2000}	δ_{J2000}	Δ_{5024}	Δ_{5053}	Gaia DR2 ID	G	$B_p - R_p$	pmRA	pmDE
Within the $3r_t$ of both clusters (filled plus signs in Figure 5)									
PS1-3PI J131558[a]	198.99365	17.59436	55.55	9.32	3938679383472421760	20.073	0.475	−1.748 ± 1.410	−0.104 ± 1.038
RS Com	198.66493	17.19691	63.35	39.62	3936953979146081792	15.564	0.530	−6.653 ± 0.096	−3.796 ± 0.068
Within the $3r_t$ of NGC 5024 (filled squares in Figure 5)									
PS1-3PI J131315[a]	198.31514	18.23614	6.33	55.74	3938773288637827712	−99.99	−99.99	−1.586 ± 1.901	−1.337 ± 1.094
…	198.02127	18.42893	19.66	76.08	3938041533584189184	−99.99[b]	−99.99[b]	−99.99	−99.99
CSS J131054[a]	197.72836	18.41797	32.28	89.96	3938090393134378752	−99.99	−99.99	6.555 ± 0.057	−7.511 ± 0.038
RR Com	197.64986	18.01958	34.28	85.72	3938004631227430144	16.318	0.490	0.347 ± 0.123	−2.788 ± 0.090
CSS J130829[a]	197.12431	17.98337	64.05	114.84	3937956660735121664	18.714	0.503	−1.405 ± 0.576	−0.072 ± 0.475
CSS J130923[a]	197.34989	18.83797	64.22	121.45	3938306378448284672	16.499	0.535	−3.361 ± 0.131	−0.028 ± 0.088
Within the $3r_t$ of NGC 5053 (filled circles in Figure 5)									
OP Com	199.55205	17.36733	89.52	32.10	3938423098479656960	16.716	0.485	−1.960 ± 0.149	−2.672 ± 0.097
OQ Com	199.67464	17.75669	86.06	32.28	3938510097337185280	14.969	0.572	1.007 ± 0.079	−5.827 ± 0.067
RT Com	199.22275	17.10860	85.22	36.05	3936916973707946752	14.016	0.550	5.249 ± 0.053	−13.564 ± 0.042
Not within the $3r_t$ of either clusters (filled triangles in Figure 5)									
Z Com	197.07614	18.54048	69.41	126.61	3938269613528220672	13.735	0.513	3.182 ± 0.049	−19.942 ± 0.046
RV Com	199.47250	18.67250	76.92	61.83	3938893311498825984	14.031	0.457	−11.983 ± 0.058	−5.711 ± 0.050
BG Com	199.93618	18.30730	97.57	59.44	3938639839708973056	15.854	0.480	−5.195 ± 0.100	−1.275 ± 0.080
CSS J131532[a]	198.88418	19.22940	73.73	92.67	3939689422341157120	18.364	0.524	−1.381 ± 0.461	−0.808 ± 0.393
CSS J131445[a]	198.68950	16.51934	102.37	74.90	3936774724391121280	15.510	0.483	−4.652 ± 0.089	−3.667 ± 0.062
CSS J132009[a]	200.03928	17.48136	111.25	54.59	3938440072190455296	18.686	0.525	−1.244 ± 0.496	−1.007 ± 0.430
…	199.83771	17.06256	113.36	56.45	3746246947188342784	18.432	0.327	−2.256 ± 0.461	−0.267 ± 0.365
PS1-3PI J131801[a]	199.50486	16.81444	109.17	57.70	3936893742228790528	18.218	0.484	−1.921 ± 0.366	−0.664 ± 0.286

Notes. The meanings of each column are same as in Table 1.
[a] PS1-3PI J131558 = PS1-3PI J131558.47 + 173539.6; PS1-3PI J131315 = PS1-3PI J131315.63 + 181410.1; PS1-3PI J131801 = PS1-3PI J131801.16 + 164851.9; CSS J130829 = CSS J130829.7 + 175900; CSS J130923 = CSS J130923.9 + 185016; CSS J131054 = CSS J131054.8 + 182504; CSS J131532 = CSS J131532.1 + 191346; CSS J131445 = CSS J131445.4 + 163109; CSS J132009 = CSS J132009.3 + 172853.
[b] The Gaia DR2 main catalog listed $G = 19.480 \pm 0.020$ and $B_P - R_p = 1.392$ for this RR Lyrae.

most promising candidate of the extra-tidal RR Lyrae is RR Com, which is located within $3r_t$ of NGC 5024. The mean brightness of this RR Lyrae is $G = 16.3176 \pm 0.0002$ mag, about ∼0.4 mag brighter than the horizontal branch of NGC 5024 (see upper right panel of Figure 5), and similar to the RR Lyrae V60 in NGC 5024 (with $G = 16.3854 \pm 0.0009$ mag). In fact, RR Com was picked up in Kundu et al. (2019) as a potential extra-tidal RR Lyrae for NGC 5024 but rejected based on the proper-motion criterion.

3. Searching for New RR Lyrae

Since none of the known RR Lyrae within our search area of ∼8 deg^2 were found to be definitive extra-tidal RR Lyrae of NGC 5024 and NGC 5053, we attempt to search for new RR Lyrae within the same area in this section. Given that RR Lyrae are high-amplitude variable stars, and the expected extra-tidal RR Lyrae would have similar brightness as those in the NGC 5024 and NGC 5053 with $G \sim 16.7$ mag (the averaged value for RR Lyrae listed in Table 1), any such new extra-tidal RR Lyrae should already have been detected from time domain all-sky surveys such as Pan-STARRS1 (as done in Sesar et al. 2017) or Gaia (Clementini et al. 2019) that can reach to a depth fainter than ∼20 mag. The fact that we did not find any extra-tidal RR Lyrae, based on the known RR Lyrae, in the previous sections indicates that most likely we will not find any new RR Lyrae around $G \sim 16.7$ mag located within our search area.

3.1. Selecting Candidates from Gaia DR2

We began the search for new RR Lyrae using the Gaia DR2 main catalog. We selected 664 stars located within the search area of ∼8 deg^2 defined in the previous section and that satisfied the conditions $16.0 < G < 17.5$ and $0.2 < (B_P - R_P) < 0.8$ (roughly bracketed the positions of expected RR Lyrae in the CMD). We further excluded those stars located within two-thirds of the tidal radius of either globular clusters, leaving 291 stars in our sample. Finally, we applied the proper-motion criterion from Kundu et al. (2019) in either the R.A. or decl. directions, but not both, leaving 79 stars (including RR Com) to be examined with ZTF light curves in the next subsection. If we enforce the Kundu et al. (2019) proper-motion criterion to be satisfied in both directions, this would leave only nine stars in the sample.

3.2. Light Curves from ZTF

The ZTF (operating 2018–2020) is a dedicated time domain wide-field synoptic sky survey aimed to explore the transient universe. ZTF utilizes the Palomar 48 inch Samuel Oschin Schmidt telescope, together with a new mosaic CCD camera,

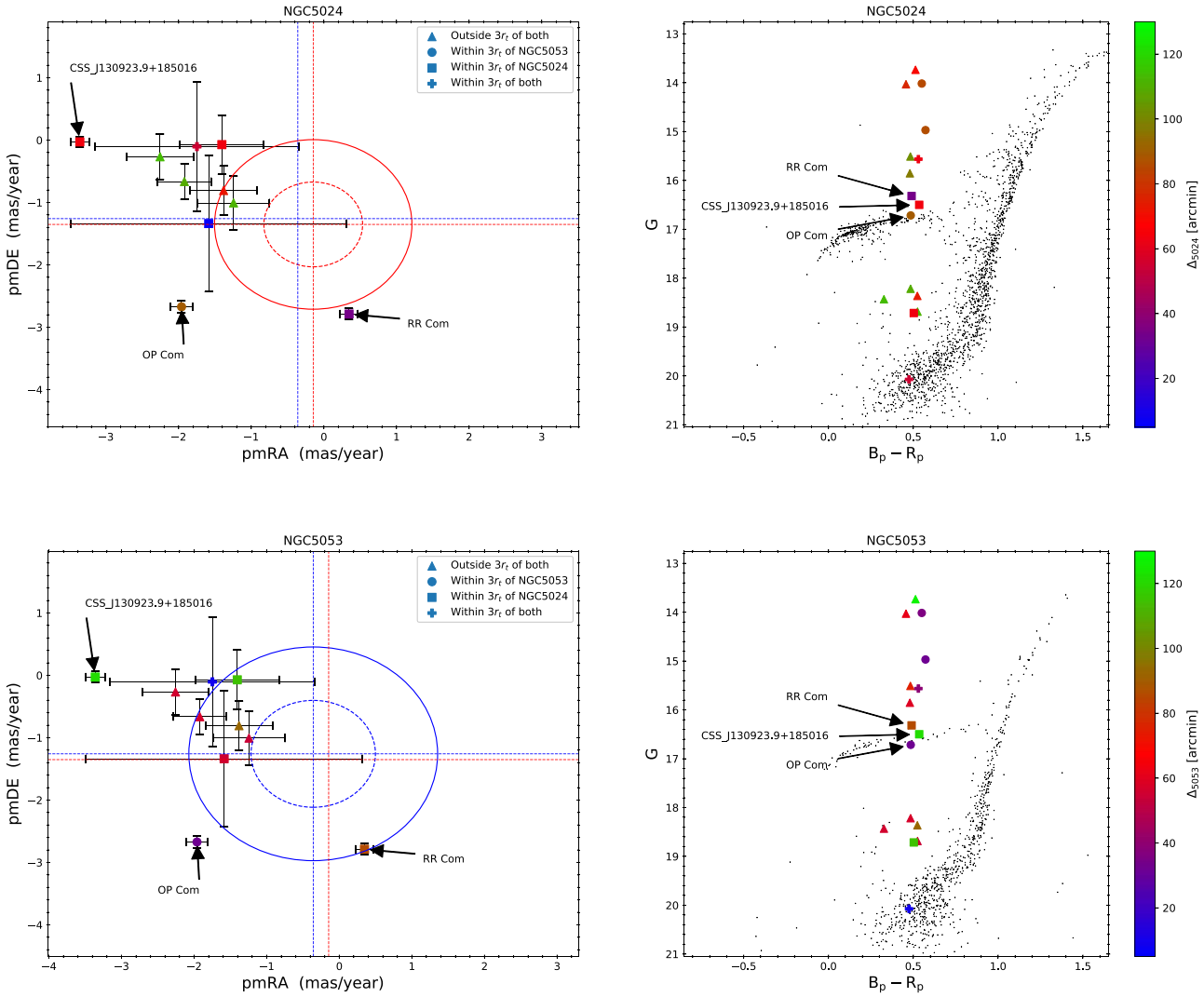

Figure 5. Left panels: comparison of the proper motions for the known RR Lyrae in Group B, as listed in Table 2. These RR Lyrae were further divided into four subgroups. Definitions of the circles and dashed lines are same as in Figure 3. Right panels: positions of these RR Lyrae on the CMD. The color bars represent the distance (Δ, in arcminute) to the center of either globular cluster.

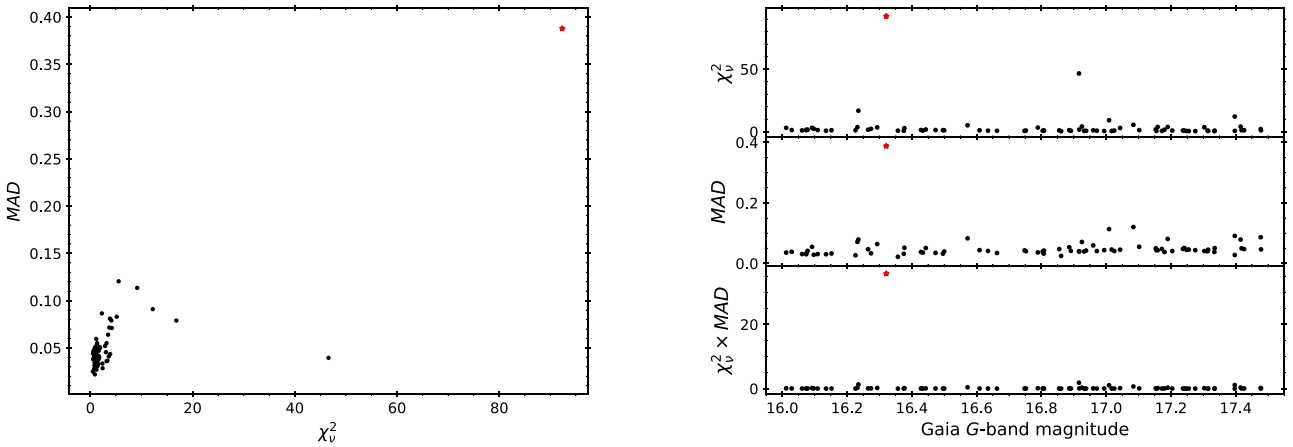

Figure 6. Left panel: MAD vs. χ^2_ν values for the 79 Gaia stars selected in Section 3.1 based on the *gri*-band ZTF light curves. Right panel: the χ^2_ν, MAD, and $\chi^2_\nu \times$ MAD values as a function of Gaia G-band magnitudes. The red starry symbols in all panels represent RR Com.

that provides a field of view of 47 squared degrees to observe the northern sky in customized *gri* filters. Further details regarding ZTF can be found in Bellm et al. (2019), Graham et al. (2019), and Dekany et al. (2020) and will not be repeated here. Imaging data taken from ZTF were processed with a dedicated reduction pipeline, as detailed in Masci et al. (2019); the final data products included reduced images and catalogs based on point-spread function (PSF) photometry.

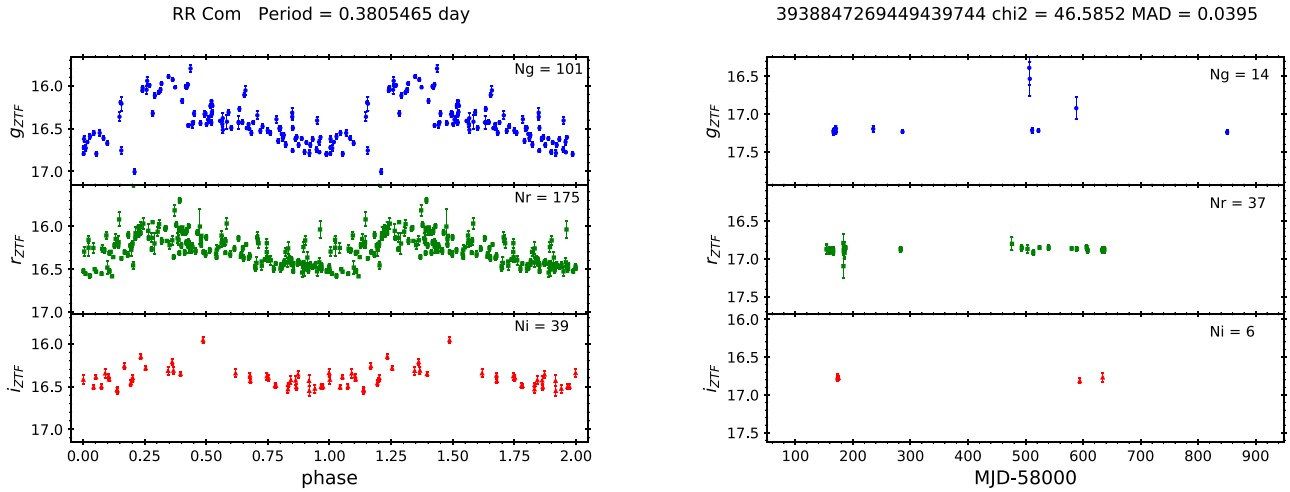

Figure 7. Left panel: ZTF light curves for RR Com, which is a known double-mode pulsator (Poleski 2014) that is simultaneously pulsating in two periods. The ZTF light curves were folded with a single period adopted from the VSX Catalog, hence the phased light curves appeared to exhibit scatters. Right panel: ZTF light curves for the star with the second highest $s \equiv \chi^2_\nu \times$ MAD value, which were affected by few outliers in the light curves. Nevertheless, it is clear that this star does not exhibit RR-Lyrae-like light curves. If the obvious outliers were removed, the χ^2_ν and MAD values were reduced to 4.1286 and 0.0340, respectively, and this star no longer belongs to the second highest s value in the sample. N is the number of data points in each light curve.

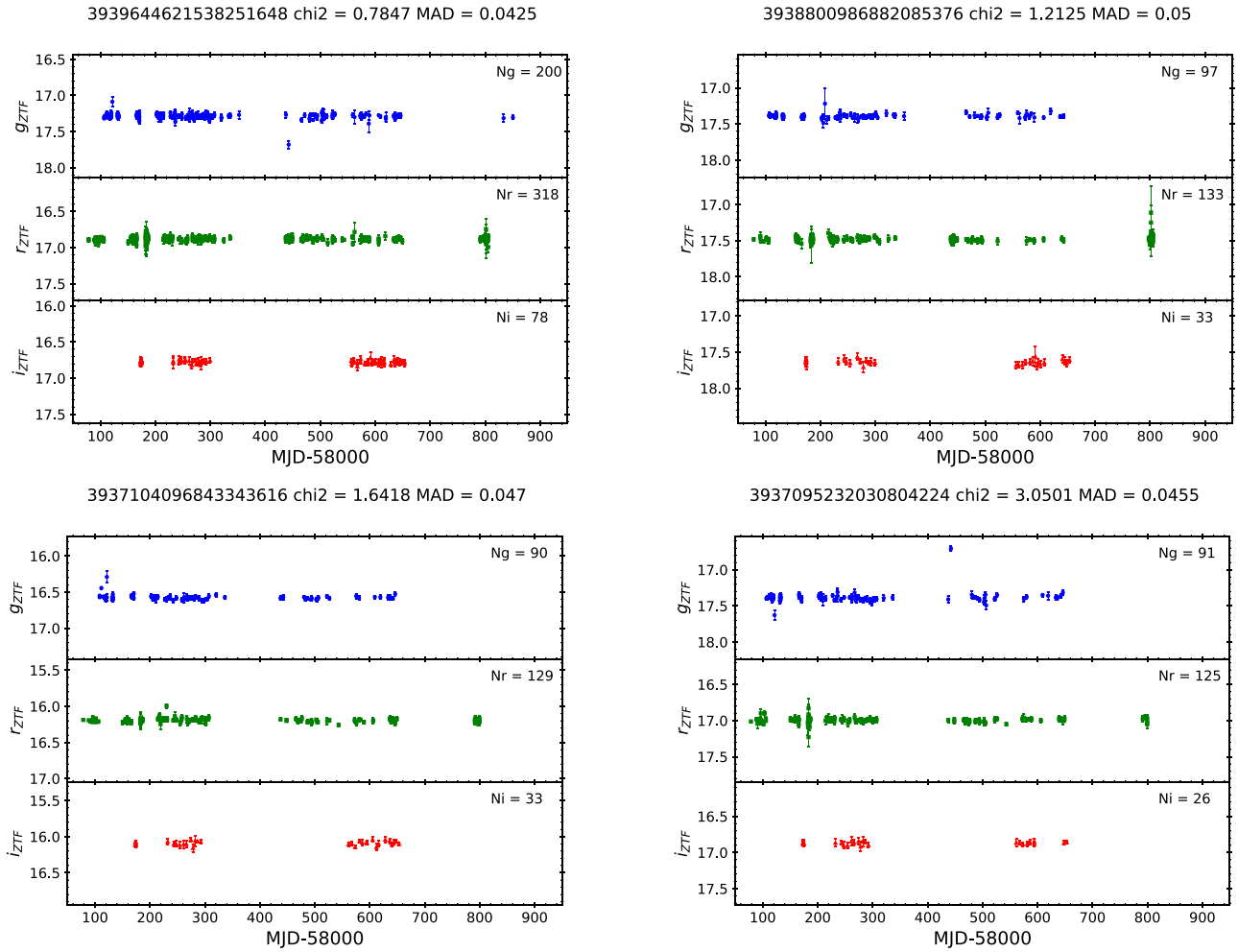

Figure 8. ZTF light curves for randomly selected stars with $s < 0.17$, where $s \equiv \chi^2_\nu \times$ MAD. N is the number of data points in each light curve.

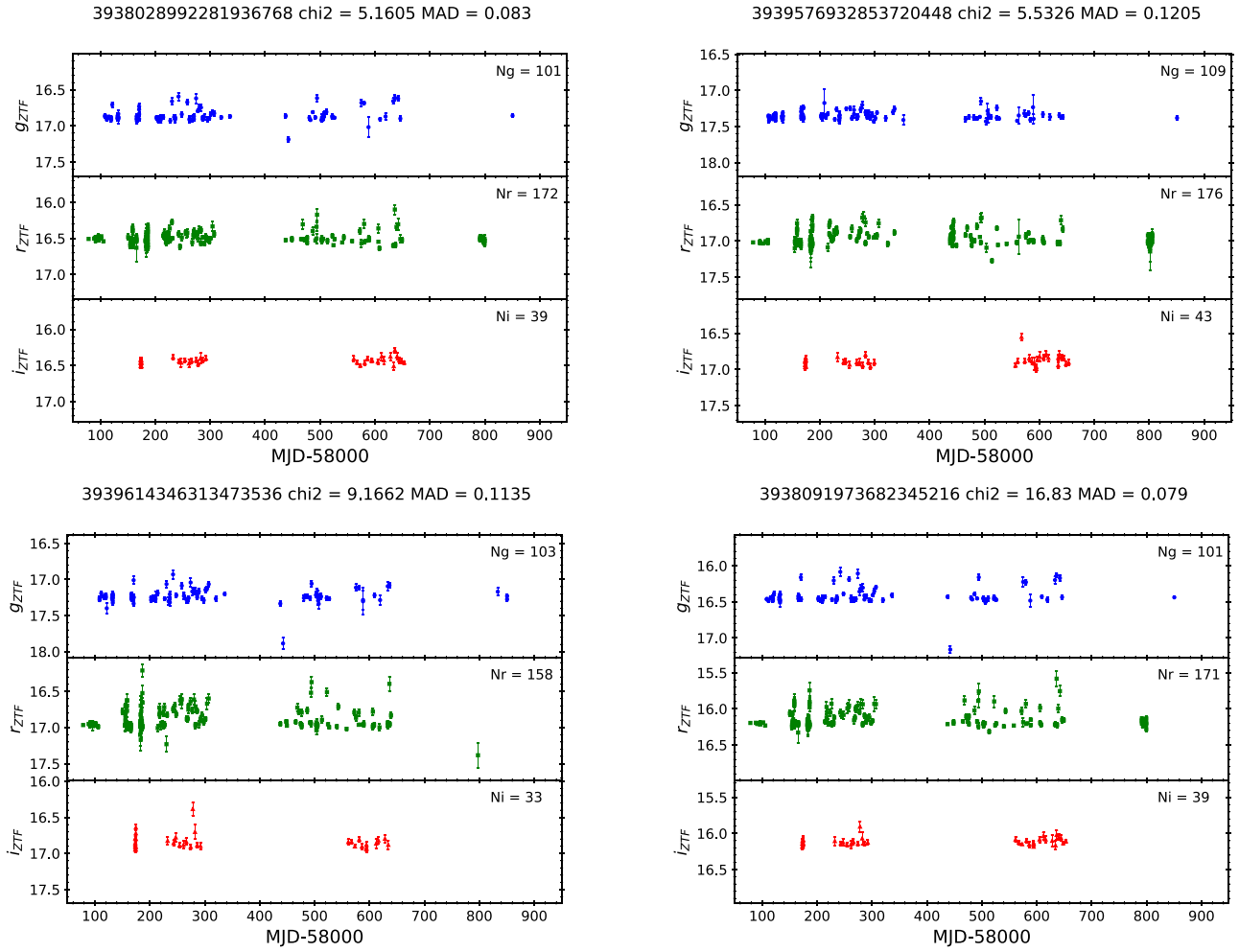

Figure 9. ZTF light curves for stars with $s > 0.17$, where $s \equiv \chi^2_\nu \times$ MAD, that exhibit variability but for which no credible period can be detected. N is the number of data points in each light curve.

Light curves of the 79 stars identified in the previous subsection were extracted from the ZTF's PSF catalogs spanning from 2017 November[16] to 2020 January. The number of data points per light curves, in the format of minimum/median/maximum, are 13/110/202 in the g band, 35/172/318 in the r band, and 5/39/78 in the i band. Following Yang & Sarajedini (2010), we calculated the χ^2_ν values for each star relative to a constant model using all gri-band data:

$$\chi^2_\nu = \frac{1}{N}\left[\sum_{j=1}^{N_g}\frac{(g_j-\bar{g})^2}{\sigma^2_{g,j}} + \sum_{j=1}^{N_r}\frac{(r_j-\bar{r})^2}{\sigma^2_{r,j}} + \sum_{j=1}^{N_i}\frac{(i_j-\bar{i})^2}{\sigma^2_{i,j}}\right],$$

where $N = N_g + N_r + N_i - 3$. To guard against outliers, we also calculated the median absolute deviation (MAD) values for the same set of light curves,

$$\mathrm{MAD} = \sum_{x=\{g,r,i\}} \mathrm{median}(|x_j - \tilde{x}|),$$

where $\tilde{x}$ is the median value of array x. The left panel of Figure 6 presents the values of MAD versus χ^2_ν, where some large values of χ^2_ν seem to be affected by outliers. The product of these two values, $\chi^2_\nu \times \mathrm{MAD} \equiv s$, appears to be a good metric to distinguish between variable and nonvariable stars, as shown in bottom right panel of Figure 6. The only known RR Lyrae among the 79 stars, RR Com, clearly stands out in this figure. Light curves for the two stars (including RR Com) with the highest values of s are presented in Figure 7. Undoubtedly, the star in the right panel of Figure 7 is not a RR Lyrae (nor a variable star of any sort).

Visually inspecting these light curves reveals that those light curves with $s < 0.17$ do not shown signs of variability. There were 65 stars with $s < 0.17$ in the sample, including the nine stars that satisfied the proper-motion criterion in Kundu et al. (2019) mentioned in the previous subsection. A few example light curves are presented in Figure 8. We searched for a periodicity on the rest of stars with $s > 0.17$, excluding RR Com, using the Lomb–Scargle periodogram implemented in the Astropy package (Astropy Collaboration et al. 2013, 2018). The periodicity search was done on the r-band light curves (as this band has the most data points) within the period range of 0.2–1.2 days, appropriate for the possible periods of RR Lyrae. Among about a dozen stars with $s > 0.17$, the majority of them do not show any periodicity, and there were four stars displaying some variability but without a convincing periodicity. Their ZTF light curves are displayed in Figure 9, and none of them are RR Lyrae.

[16] Part of the data were taken during the ZTF commissioning phase from 2017 November to 2018 March.

4. Conclusion

In this work, we re-evaluated the claim of Kundu et al. (2019) that there are five extra-tidal RR Lyrae associated with globular cluster NGC 5024. Four of these RR Lyrae were known members of a nearby globular cluster NGC 5053. The remaining extra-tidal RR Lyrae, V48 of NGC 5024, could either be an extra-tidal RR Lyrae of NGC 5024 or not—depending on the adopted tidal radius of NGC 5024. One of the criteria employed in Kundu et al. (2019) is such that extra-tidal RR Lyrae should be located outside the two-thirds of the tidal radius for a given globular cluster. Other similar work in literature, however, adopted the criterion of one tidal radius to select the extra-tidal RR Lyrae (Kunder et al. 2018; Minniti et al. 2018). If the criterion of one tidal radius is adopted, then V48 will no longer be an extra-tidal RR Lyrae of NGC 5024.

Besides the RR Lyrae that were known members of NGC 5024 and NGC 5053 from Clement's Catalog, we compiled a list of known RR Lyrae within an area of $\sim$8 deg^2 from the literature. Using the similar selection criteria as in Kundu et al. (2019), together with the Gaia DR2 data, none of these known RR Lyrae were found to be extra-tidal RR Lyrae of either globular clusters. Finally, using Gaia DR2 data, we selected stars within our search area but outside the two-thirds of the tidal radii of both globular clusters that fall in the range of $16.0 < G < 17.5$ and $0.2 < (B_P - R_P) < 0.8$, as well as satisfied the proper-motion criterion from Kundu et al. (2019) in either direction. A further variability and periodicity analysis of these stars with the ZTF light curves data revealed that none of them were new RR Lyrae. Therefore, we have concluded there were no extra-tidal RR Lyrae for either NGC 5024 or NGC 5053 within our search area of $\sim$8 deg^2 that covered both globular clusters.

We thank the useful discussions and comments from T. de Boer, P. Mroz, and an anonymous referee which improved the manuscript. We thank the funding from Ministry of Science and Technology (Taiwan) under the contract 107-2119-M-008-014-MY2, 107-2119-M-008-012, and 108-2628-M-007-005-RSP.

Based on observations obtained with the Samuel Oschin Telescope 48 inch and the 60 inch Telescope at the Palomar Observatory as part of the Zwicky Transient Facility project. Major funding has been provided by the U.S. National Science Foundation under grant No. AST-1440341 and by the ZTF partner institutions: the California Institute of Technology, the Oskar Klein Centre, the Weizmann Institute of Science, the University of Maryland, the University of Washington, Deutsches Elektronen-Synchrotron, the University of Wisconsin-Milwaukee, and the TANGO Program of the University System of Taiwan.

This work has made use of data from the European Space Agency (ESA) mission Gaia (https://cosmos.esa.int/gaia), processed by the Gaia Data Processing and Analysis Consortium (DPAC, https://cosmos.esa.int/web/gaia/dpac/consortium). Funding for the DPAC has been provided by national institutions, in particular the institutions participating in the Gaia Multilateral Agreement.

This research has made use of the SIMBAD database and the VizieR catalog access tool, operated at CDS, Strasbourg, France. This research has made use of the International Variable Star Index (VSX) database, operated at AAVSO, Cambridge, Massachusetts, USA.

This research made use of Astropy,[17] a community-developed core Python package for Astronomy (Astropy Collaboration et al. 2013, 2018).

Facilities: Gaia, PO:1.2 m.

Software: Astropy package (Astropy Collaboration et al. 2013, 2018), Astroquery (Ginsburg et al. 2019).

Appendix A
Constructing the Proper Motion and CMDs for the Clusters

We utilize the proper motions and color–magnitude diagrams (PMD and CMD, respectively) to evaluate the probable membership of the selected RR Lyrae and candidates (as described in Section 2) in the vicinity of the two globular clusters studied in this work. More precisely, these diagrams, constructed using the data in Gaia DR2 catalog, are used to reject RR Lyrae and candidates that are obviously not members of the clusters. Sources within 1 tidal radius of each globular cluster were queried from the Gaia DR2 main catalog (Gaia Collaboration et al. 2018a), and the corresponding PMD and CMD are shown in Figure A1. As can be seen from the figure, there are large scatters in the PMD and many outliers in the CMD, which are probably foreground or background sources. Since our goal is not to establish the cluster membership of each Gaia source, but construct a clean CMD to be compared with the RR Lyrae and candidates, we adopted a simple criterion to select the Gaia sources. For each Gaia source, we calculated $\Delta_{\rm PM} = [({\rm pmRA} - {\rm pmRA}_c)^2 + ({\rm pmDE} - {\rm pmDE}_c]^2)^{1/2}$, where pmRA and pmDE are proper motions for each source in R. A. and decl., respectively, and the subscript $_c$ represents the measured proper motions of the clusters (Gaia Collaboration et al. 2018b). Only those sources with $\Delta_{\rm PM} < {\rm pmT}/2$ are kept as the clean sample, where pmT is the quadrature sum of pmRA$_c$ and pmDE$_c$. The clean CMDs of NGC 5024 and NGC 5053 are presented in Section 2.

[17] http://astropy.org

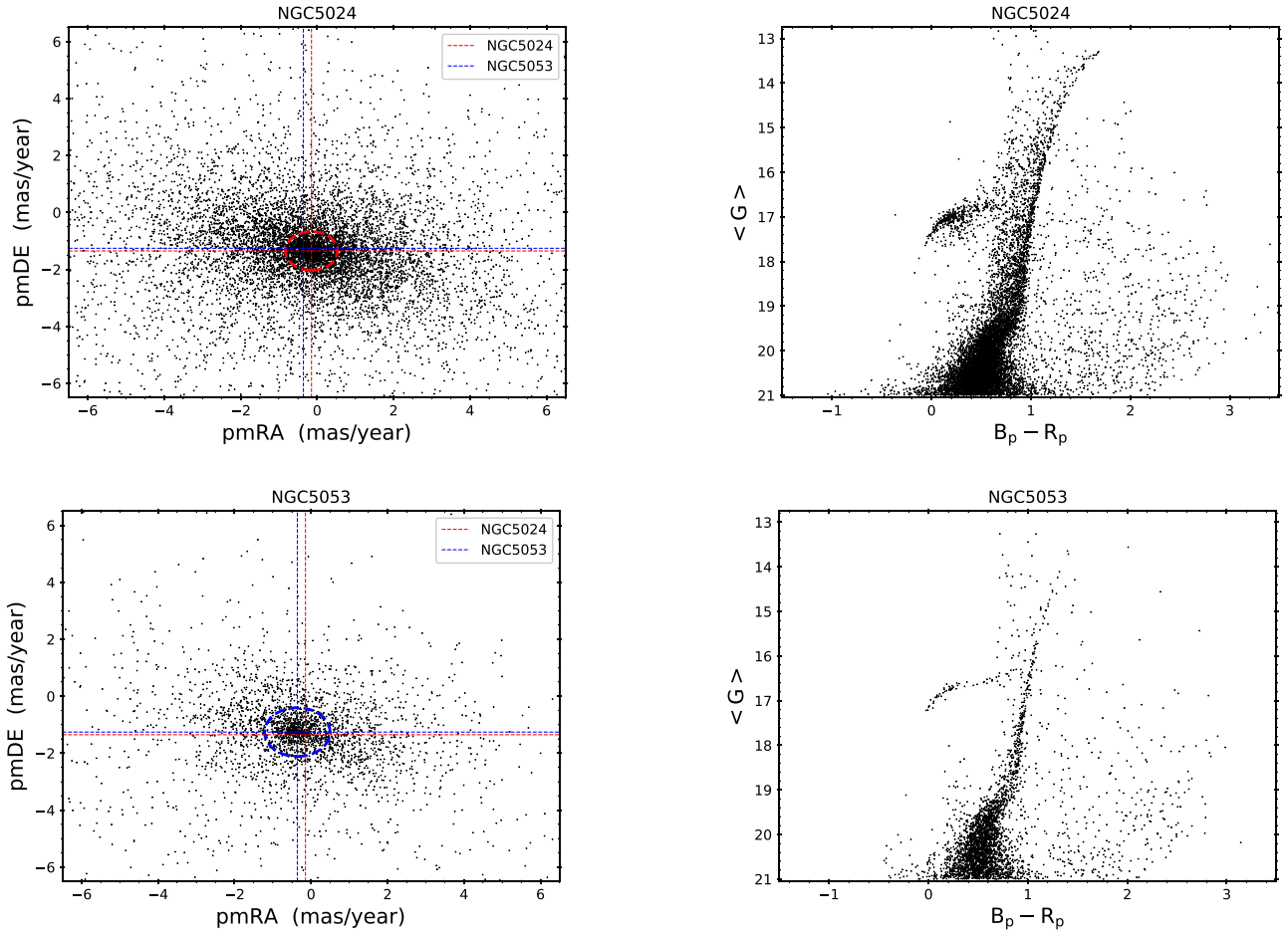

Figure A1. Gaia sources, queried from the DR2 main catalog, located within 1 tidal radius of NGC 5024 and NGC 5053. The left panels present the proper motions of these sources, while the right panels are the corresponding CMD. The dashed lines in left panels are the measured proper motions for each cluster adopted from Gaia Collaboration et al. (2018b), while the dashed circles represent the selection criterion of $\Delta_{\rm PM} = {\rm pmT}/2$ (only sources within the circles were be used to construct the clean CMD).

Appendix B
Light Curves for Two Misidentified RR Lyrae

We have examined the ZTF light curves for RR Lyrae listed in Table 2, and found that two of them do not display RR-Lyrae-like light curves. These two putative RR Lyrae are PS1-3PI J131315.63 + 181410.1 (abbreviated as PS1-3PI J131315) and Gaia DR2 ID 3938041533584189184, but we classify them as non-RR Lyrae. Other RR Lyrae in Table 2 display the light-curve shapes expected for ab- or c-type RR Lyrae after folding the ZTF light curves with their published periods.

PS1-3PI J131315. This star is identified in Sesar et al. (2017) with final classification scores of `S3ab=0.93` and `S3c=0.02`, suggesting this star has a high probability of being an ab-type RR Lyrae. The period of PS1-3PI J131315 is found to be 0.6386368 days (Sesar et al. 2017). However the Lomb–Scargle periodogram applied to its *r*-band ZTF light curve did not reveal any significant peak between 0.2 and 1.2 days (see left panel of Figure B1). The folded ZTF light curves for this star, either with the published period or the best period (corresponding to the highest peak in the Lomb–Scargle periodogram), as shown in right panel of Figure B1, do not resemble those of ab-type RR Lyrae.

3938041533584189184. This star is identified in Rimoldini et al. (2019) as an ab-type RR Lyrae with a `best_class_score=0.6279`, but there is no period found for this star. We ran the Lomb–Scargle periodogram on the ZTF *r*-band light curve for this star, and no significant peak was found between 0.2 and 1.2 days. The Lomb–Scargle periodogram and the folded ZTF light curves with the best period are displayed in Figure B2. Clearly, this star is not an ab-type RR Lyrae.

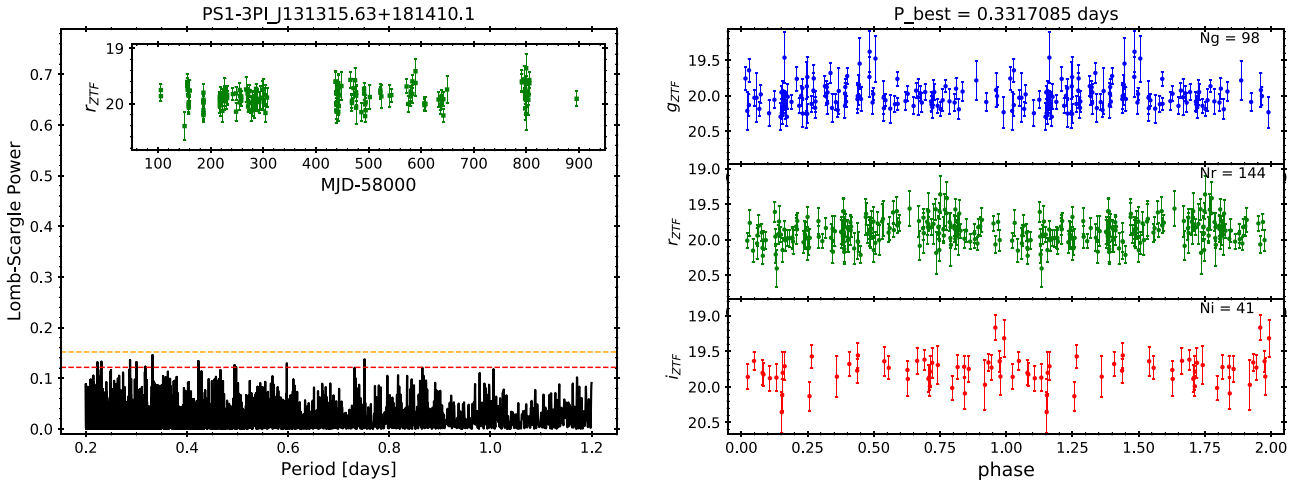

Figure B1. Left panel: the Lomb–Scargle periodogram for PS1-3PI J131315 based on the *r*-band ZTF light curve, shown in the inset figure. The horizontal red and orange dashed lines represent the false-alarm probability of 0.1 and 0.01, respectively. Right panel: folded ZTF *gri*-band light curves with the best period, corresponding to the highest peak in the Lomb–Scargle periodogram. Note that the best period does not necessary represent the true period.

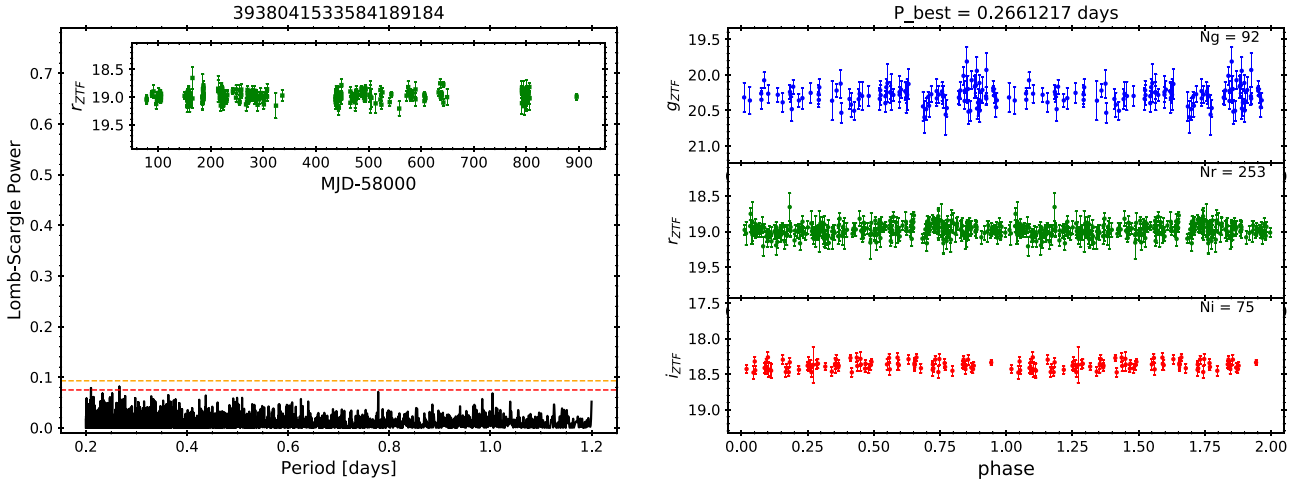

Figure B2. Same as Figure B1, but for the star with the Gaia DR2 ID 3938041533584189184.

ORCID iDs

Chow-Choong Ngeow https://orcid.org/0000-0001-8771-7554
Matthew J. Graham https://orcid.org/0000-0002-3168-0139
David L. Kaplan https://orcid.org/0000-0001-6295-2881
Thomas Kupfer https://orcid.org/0000-0002-6540-1484
Ashish Mahabal https://orcid.org/0000-0003-2242-0244
Frank J. Masci https://orcid.org/0000-0002-8532-9395
Reed Riddle https://orcid.org/0000-0002-0387-370X
Ben Rusholme https://orcid.org/0000-0001-7648-4142

References

Arellano Ferro, A., Figuera Jaimes, R., Giridhar, S., et al. 2011, MNRAS, 416, 2265
Astropy Collaboration, Price-Whelan, A. M., Sipőcz, B. M., et al. 2018, AJ, 156, 123
Astropy Collaboration, Robitaille, T. P., Tollerud, E. J., et al. 2013, A&A, 558, A33
Baumgardt, H., & Makino, J. 2003, MNRAS, 340, 227
Beccari, G., Lanzoni, B., Ferraro, F. R., et al. 2008, ApJ, 679, 712
Bellm, E. C., Kulkarni, S. R., Graham, M. J., et al. 2019, PASP, 131, 018002
Belokurov, V., Evans, N. W., Irwin, M. J., et al. 2006, ApJL, 637, L29
Capuzzo Dolcetta, R., di Matteo, P., & Miocchi, P. 2005, AJ, 129, 1906
Chun, S.-H., Kim, J.-W., Sohn, S. T., et al. 2010, AJ, 139, 606
Clement, C. M. 2017, EPJWC, 152, 01021
Clement, C. M., Muzzin, A., Dufton, Q., et al. 2001, AJ, 122, 2587
Clementini, G., Ripepi, V., Molinaro, R., et al. 2019, A&A, 622, A60
Combes, F., Leon, S., & Meylan, G. 1999, A&A, 352, 149
de Boer, T. J. L., Gieles, M., Balbinot, E., et al. 2019, MNRAS, 485, 4906
Dehnen, W., Odenkirchen, M., Grebel, E. K., et al. 2004, AJ, 127, 2753
Dekany, R., Smith, R. M., Riddle, R., et al. 2020, PASP, 132, 038001
Fellhauer, M., Evans, N. W., Belokurov, V., et al. 2007, MNRAS, 380, 749
Fernández-Trincado, J. G., Vivas, A. K., Mateu, C. E., et al. 2015, A&A, 574, A15
Gaia Collaboration, Brown, A. G. A., Vallenari, A., et al. 2018a, A&A, 616, A1
Gaia Collaboration, Helmi, A., van Leeuwen, F., et al. 2018b, A&A, 616, A12
Gaia Collaboration, Prusti, T., de Bruijne, J. H. J., et al. 2016, A&A, 595, A1
Ginsburg, A., Sipőcz, B. M., Brasseur, C. E., et al. 2019, AJ, 157, 98
Graham, M. J., Kulkarni, S. R., Bellm, E. C., et al. 2019, PASP, 131, 078001
Grillmair, C. J. 2019, ApJ, 884, 174
Harris, W. E. 1996, AJ, 112, 1487
Harris, W. E. 2010, arXiv:1012.3224
Hozumi, S., & Burkert, A. 2015, MNRAS, 446, 3100
Ibata, R. A., Lewis, G. F., Thomas, G., et al. 2017, ApJ, 842, 120

Jordi, K., & Grebel, E. K. 2010, A&A, 522, A71
Kharchenko, N. V., Piskunov, A. E., Schilbach, E., et al. 2013, A&A, 558, A53
Kunder, A., Mills, A., Edgecomb, J., et al. 2018, AJ, 155, 171
Kundu, R., Minniti, D., & Singh, H. P. 2019, MNRAS, 483, 1737
Lauchner, A., Powell, W. L., & Wilhelm, R. 2006, ApJL, 651, L33
Lee, K. H., Lee, H. M., & Sung, H. 2006, MNRAS, 367, 646
Lehmann, I., & Scholz, R.-D. 1997, A&A, 320, 776
Masci, F. J., Laher, R. R., Rusholme, B., et al. 2019, PASP, 131, 018003
McLaughlin, D. E., & van der Marel, R. P. 2005, ApJS, 161, 304
Minniti, D., Fernández-Trincado, J. G., Ripepi, V., et al. 2018, ApJL, 869, L10
Montuori, M., Capuzzo-Dolcetta, R., di Matteo, P., et al. 2007, ApJ, 659, 1212
Myeong, G. C., Jerjen, H., Mackey, D., et al. 2017, ApJL, 840, L25
Navarrete, C., Belokurov, V., & Koposov, S. E. 2017, ApJL, 841, L23
Nemec, J. M. 2004, AJ, 127, 2185
Niederste-Ostholt, M., Belokurov, V., Evans, N. W., et al. 2010, MNRAS, 408, L66
Odenkirchen, M., Grebel, E. K., Rockosi, C. M., et al. 2001, ApJL, 548, L165
Peterson, C. J., & King, I. R. 1975, AJ, 80, 427
Poleski, R. 2014, PASP, 126, 509
Price-Whelan, A. M., Mateu, C., Iorio, G., et al. 2019, AJ, 158, 223
Rimoldini, L., Holl, B., Audard, M., et al. 2019, A&A, 625, A97
Rockosi, C. M., Odenkirchen, M., Grebel, E. K., et al. 2002, AJ, 124, 349
Sarajedini, A., & Milone, A. A. E. 1995, AJ, 109, 269
Sesar, B., Hernitschek, N., Mitrović, S., et al. 2017, AJ, 153, 204
Sollima, A., Martínez-Delgado, D., Valls-Gabaud, D., et al. 2011, ApJ, 726, 47
Trager, S. C., King, I. R., & Djorgovski, S. 1995, AJ, 109, 218
Vivas, A. K., & Zinn, R. 2006, AJ, 132, 714
Vivas, A. K., Zinn, R., Andrews, P., et al. 2001, ApJL, 554, L33
Watson, C. L., Henden, A. A., & Price, A. 2006, SASS, 25, 47
Wu, C., Qiu, Y. L., Deng, J. S., et al. 2005, AJ, 130, 1640
Yang, S.-C., & Sarajedini, A. 2010, ApJ, 708, 293
Yim, K.-J., & Lee, H. M. 2002, JKAS, 35, 75